Contributed paper

OPTO-ELECTRONICS REVIEW **11**(2), 85–91 (2003)

High power quantum cascade lasers grown by GasMBE

M. RAZEGHI* and S. SLIVKEN

Centre for Quantum Devices, Department of Electrical and Computer Engineering,
Northwestern University, Evanston, Illinois 60208, USA

This paper is a brief summary of the technological development and state-of-the-art performance of quantum cascade lasers (QCLs) produced at the Centre for Quantum Devices. Laser design will be discussed, as well as experimental details of device fabrication. Recent work has focused on the development of high peak and average power QCLs emitting at room temperature and above. Scaling of the output is demonstrated by increasing the number of emitting regions in the waveguide core. At λ = 9 μm, over 7 W of peak power has bee demonstrated at room temperature for a single diode, with an average power of 300 mW at 6% duty cycle. At shorter wavelengths, laser development includes the use of highly strain-balanced heterostructures in order to maintain a high conduction band offset and minimize leakage current. At λ = 6 μm, utilizing a high reflective coating and epilayer-down mounting of the laser, we have demonstrated 225 mW of average power from a single facet at room temperature. Lastly, these results are put in the perspective of other reported results and possible future directions are discussed.

Keywords: quantum cascade laser, high power, molecular beam epitaxy.

1. Introduction

Compact, high-power lasers in the mid-to far-infrared wavelength range (3–20 μm) are in great demand for many laser-based applications areas such as free-space communication, chemical sensing, and medicine. Gas lasers and parametric oscillators are bulky and require precise alignment of specialized optics. The semiconductor laser, on the other hand, is inherently compact and durable, with an internal optical cavity and low voltage/current operation. Up until recently, the only commercially available semiconductor laser in the mid- and far-infrared wavelength range has been based on lead-salt technology, which has both low power output and high sensitivity to temperature.

The quantum cascade laser (QCL) is a unipolar semiconductor laser [1]. Rather than relying on intrinsic band gaps, quantum effects are exploited in order to produce designer energy levels and transitions within the conduction band of a complex heterostructure. The benefit of this approach is a widely variable transition energy dictated primarily by layer thicknesses. Typical emission wavelengths vary from 3.4–24 μm. Further, because the primary limitation to radiative efficiency is based on phonons rather than Auger processes, the device performance is much less sensitive to temperature change than competing semiconductor technologies. The primary requisite is a heterostructure with a large conduction band offset and well-controlled interfaces. In other words, it now becomes practical to use mature GaAs- and InP-based technology to produce long wavelength emitters.

The last hurdle to overcome, in order to compete more directly with gas and solid state lasers, is output power. As remote systems benefit from high power, this figure of merit helps determine the range and usefulness of the laser source. Towards this end, this paper will address the state-of-the-art for high peak and high average power quantum cascade laser technology demonstrated at the Centre for Quantum Devices.

2. Quantum cascade laser design

The QCL is based on electron transitions within semiconductor nanostructures. The emitting structure of the QCL can be varied from a single quantum well to a complex chirped superlattice. In all cases, the wavelength of emitted light is primarily determined by the thickness of the semiconductor layers rather than their bandgap. The design of the active region is complex, and relies on optimising the wavefunctions for a long carrier lifetime and high dipole matrix element. The structure must also be optimised for high current density throughput. By utilizing resonant tunneling and miniband conduction, a special bridge, or injector region, can be designed to connect adjacent active regions. These dual regions make up one period, or stage, of the QCL, and can be exploited to connect together a cascade of quantum well or superlattice emitters. Representative conduction band and cascade schematics are shown in Fig. 1. Wavefunctions are modelled numerically under the envelope function approximation (EFA). An energy dependent effective mass is incorporated into the calculation as a result of band nonparabolicity.

*e-mail: razeghi@ece.northwestern.edu

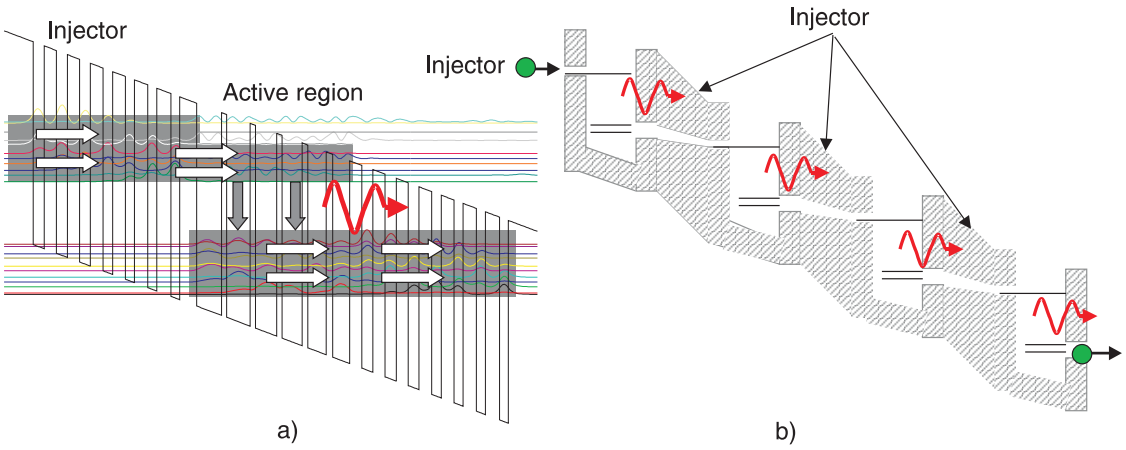

Fig. 1. Superlattice quantum cascade laser conduction band schematic (a) and cascade operation of serially stacked active/injector stages (b).

The cascade nature of the QCL provides an elegant way to scale the output power of a single device. Above threshold, multiple photons can be emitted for every injected electron. By increasing the number of periods, the overall power output should increase. However, the true potential of the device is limited by material quality. If the material is non-uniform, it is difficult to keep the peak gain at a constant wavelength. This is due to variations in local temperature, electric field, dopant distribution, and layer thickness.

Thermal considerations are also critical. While scaling the number of stages can increase the peak output power, the large number of interfaces can lead to a large device thermal resistance, which limits the maximum average power output and continuous wave operating temperature. Thermal backfilling of electrons from an injector into the lower levels of the previous active region decreases the population inversion, leading to lower efficiency and higher threshold current density. For this reason, the active and injector regions need to be designed to accommodate large lattice (and larger electron) temperatures. Internally, this effect is minimised by utilizing a wide injector miniband. This miniband, while still offering a clear conduction path, acts also as a deep reservoir, giving a significant barrier to backfilling.

Doping of the injector region is necessary in order to maintain a steady-state population inversion as dictated by charge neutrality. The level of doping must be carefully optimised to given minimal absorption and leakage, yet supply enough carrier to achieve population inversion and accommodate a large current density through the structure.

As the quantum cascade laser often emits at longer wavelengths than traditional semiconductor lasers, special considerations must be made during laser waveguide design. One such consideration is free carrier absorption. Emitted light, instead of being collected, is absorbed by plasma-like oscillations of free carriers in the semiconductor. The absorption coefficient is proportional to the number of free-carriers and is strongly dependent on the frequency of light. A simplified expression for the absorption coefficient is given by [2]

$$\alpha_{fc}(\omega) = \frac{\varepsilon_\infty \omega_p^2 \gamma_{pl}}{n_r c(\omega^2 + \gamma_{pl}^2)} = \frac{4\pi N_d e^2 \gamma_{pl}}{n_r m^* c(\omega^2 + \gamma_{pl}^2)}, \tag{1}$$

where ε_∞ is the high frequency permittivity, ω_p is the plasma frequency of the material, γ_{pl} is the characteristic scattering rate of electrons, n_r is the refractive index, c is the speed of light, ω is the frequency, N_d is the concentration of carriers, e is the electronic charge of the carriers, and m^* is the electron effective mass**.** In the mid- to far-infrared, the absorption coefficient can be experimentally fitted to give a λ dependence [2,3]. In order to reduce the loss, the doping should be kept to a minimum wherever the photon density is high.

Another consideration that is particularly important is coupling of the laser TM modes (primary emission modes for an intersubband laser) to the surface plasmon mode [3]. The surface plasmon mode is very lossy, and exists at the interface between the contact metal and the cap layer of the waveguide. In order to reduce the coupling to the surface plasmon mode, a thick cladding and a highly doped cap layer are used. The cladding allows the fundamental optical mode to decay slowly and preserve a low beam divergence. The cap layer is highly doped and attenuates the optical mode before it encounters the metal surface. This design has been extremely successful at longer wavelengths, as evidenced by extremely low threshold current densities.

3. Strain-balanced laser design

Unlike lasers designed for the 8–24 μm wavelength range, carrier confinement at shorter wavelengths ($\lambda < 6$ μm) is a serious problem. For an intersubband laser, carrier confinement is facilitated by use of a heterostructure with a large conduction band offset (ΔE_c), as shown in Fig. 2.

The maximum conduction band offset in the lattice matched $Ga_{0.47}In_{0.53}As/Al_{0.48}In_{0.52}As/InP$ heterostructure is only 510 meV. Accounting for substantial lower energy

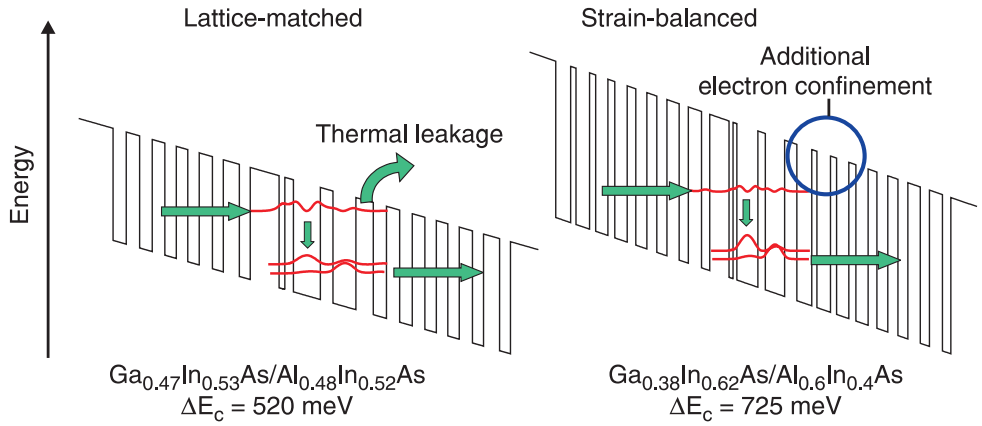

Fig. 2. Conduction band diagram for (a) lattice-matched and (b) strain-balanced quantum cascade lasers. Inside the active region, the modulus squared of the electron wavefunction is displayed. Arrows indicate electron current. The strain-balanced design offers a higher conduction band offset for the heterostructure and, therefore, lower electron leakage into the continuum.

level confinement energies, this limits operation to $\lambda > 4.5$ μm. In order to reduce current leakage and design for even shorter wavelength lasers, strain-balancing must be employed. This technique, while demonstrated in the laboratory, has not yet been fully explored in terms of laser performance and durability.

The key to a successful strain-balanced design is to incorporate strained heterostructures which intrinsically have higher conduction band offsets (ΔE_c). However, in order to avoid unwanted misfit dislocations, the net strain should be zero. This is accomplished by proper selection of materials and accurate control over layer composition. For the $Ga_xIn_{1-x}As/Al_yIn_{1-y}As$ QCL, x and y are chosen such that compressive strain of the $Ga_xIn_{1-x}As$ quantum wells are balanced throughout the entire device with an equal and opposite tensile strain due to $Al_yIn_{1-y}As$ quantum barriers. The ΔE_c can be calculated using a method such as model solid theory [4]. Using this technique, the conduction band offset can be increased at least 50% with near zero net strain.

4. Material growth, characterization and laser fabrication

One benefit of gas-source molecular beam epitaxy (GasMBE) is the ability to grow a wide range of As- and P-containing materials in a single epitaxial run. This means that we can choose the best materials for the active layers and waveguide, regardless of the composition. AsH_3 and PH_3 are precursors for As and P respectively, and are cracked at 900°C. Elemental effusion cells are used to provide Ga, In, and Al. Si is used as the n-type dopant.

Structural quality, layer thickness, and interface smoothness are very important to QCL device performance. Typical x-ray diffraction for lattice-matched and strain-compensated laser structures (Fig. 3) exhibit clear satellite peaks over 4 degrees. X-ray simulation shows excellent agreement between the ideal and as-grown diffraction spectra. Surface quality is confirmed with atomic force microscopy (AFM). Typical strain-compensated laser structures exhibit an rms roughness of less than 0.2 nm

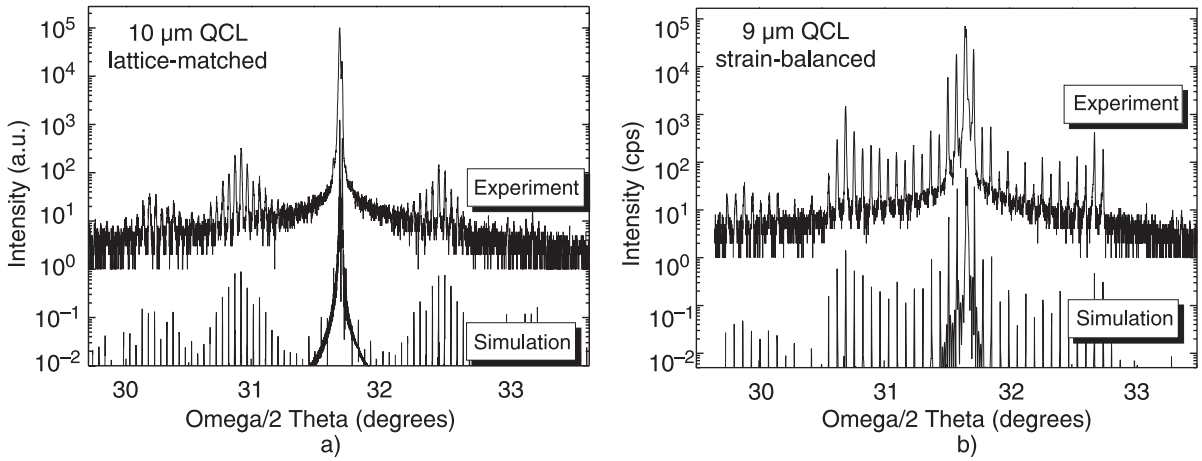

Fig. 3. Typical omega/2 theta x-ray diffraction for (a) lattice-matched and (b) strain-balanced quantum cascade lasers. Simulated diffraction plotted along with experimental data shows the excellent epitaxial control and material quality.

over a 50 μm square area. Excellent uniformity has been demonstrated in-house for a two-inch wafer.

Doping was accurately controlled, and was measured using electrochemical capacitance-voltage (ECV) profiling. The doping profile for a laser structure is shown in Fig. 4. While not accurate enough to measure the modulation doping in the injector, a good average doping can be recorded for the active layers as a whole.

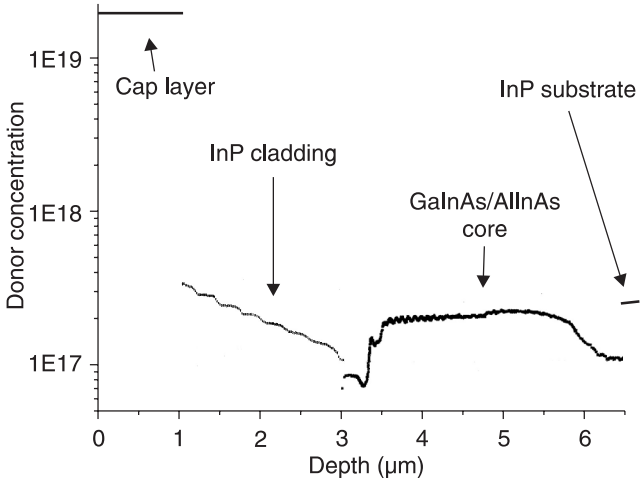

Fig. 4. Electrochemical capacitance-voltage measurements for a quantum cascade laser structure. Although the active layers are modulation doped during growth, the observed data for the core is an average donor concentration, limited by the resolution of the profiler.

After characterization of the wafers, they are processed into lasers as double-channel ridge waveguides, for efficient optical and electrical confinement. Definition of the ridge along the $[1\bar{1}0]$ direction is performed using photolithography and wet chemical etching in $HBr:HCl:H_2O_2:H_2O$ (10:5:1:50). Current is injected only through the opening in the top of the centre ridge, which is laterally insulated with a dielectric such as SiO_2. An example is given in Fig. 5.

5. Long wavelength (8–16 μm) quantum cascade lasers

The first uncooled demonstration of an 8.5 μm QCL was in 1997 by Sirtori et al. [5]. Since then there have many reports, including many high power results [6] and reduced threshold current density at room temperature [7]. Recently, by employing a buried ridge structure, combined with epilayer-down mounting and mirror coating, room temperature continuous operation was demonstrated at 9 μm [8].

Recent efforts have focused on increasing the peak and average output power of our QCLs at high temperatures. By scaling the number of periods in a superlattice-based design, power scaling has indeed been demonstrated, as shown in Fig. 6. No clear saturation is observed at 9 μm, but the power does depend somewhat on wavelength--dependent loss in the waveguide.

For a 75 period device operating at room temperature, the total device peak power is over 7 W at 3.26 A, with a threshold current density of 1.4 kA/cm^2 and slope efficiency of 4.4 W/A, as shown in Fig. 6(b). In terms of total optical efficiency this translates to 32 emitted photons per injected electron. At the maximum power, and an operating voltage of 22 V, the power conversion efficiency is ~9%. All of these results are the best reported to date for a mid-infrared semiconductor laser. The same device is able to operate up to 425 K (limit of testing setup) with 2.4 W peak output. In terms of beam quality, the results are fairly typical for state-of-the-art QCLs. Even with such a thick core, this laser shows a single lobe elliptical far-field pattern with angular width (for half-maximum intensity) of 63° and 30° in the perpendicular and parallel directions respectively. These results are indicative of a low-loss wave-

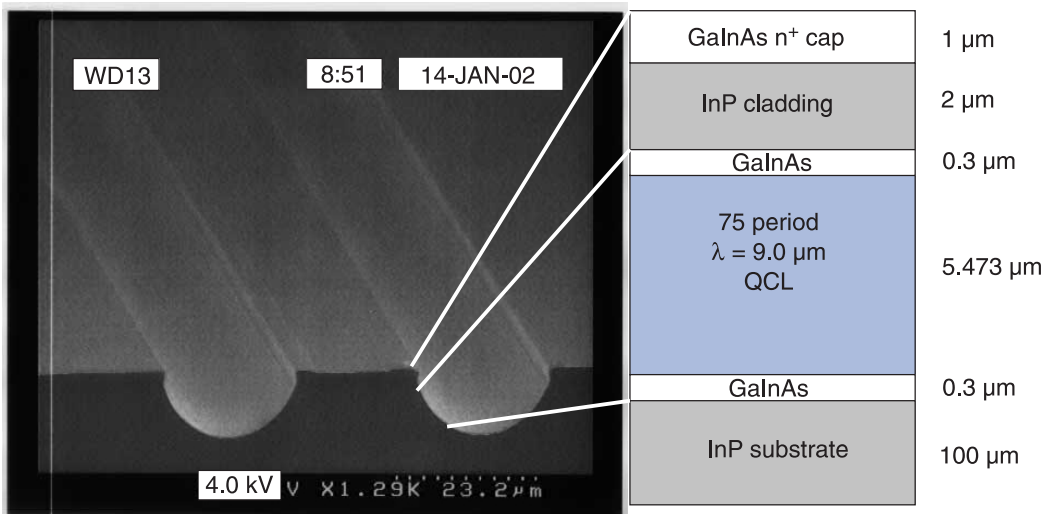

Fig. 5. Oblique scanning electron microscope image of a 75 QCL double-channel ridge waveguide. The waveguide structure is shown schematically on the right.

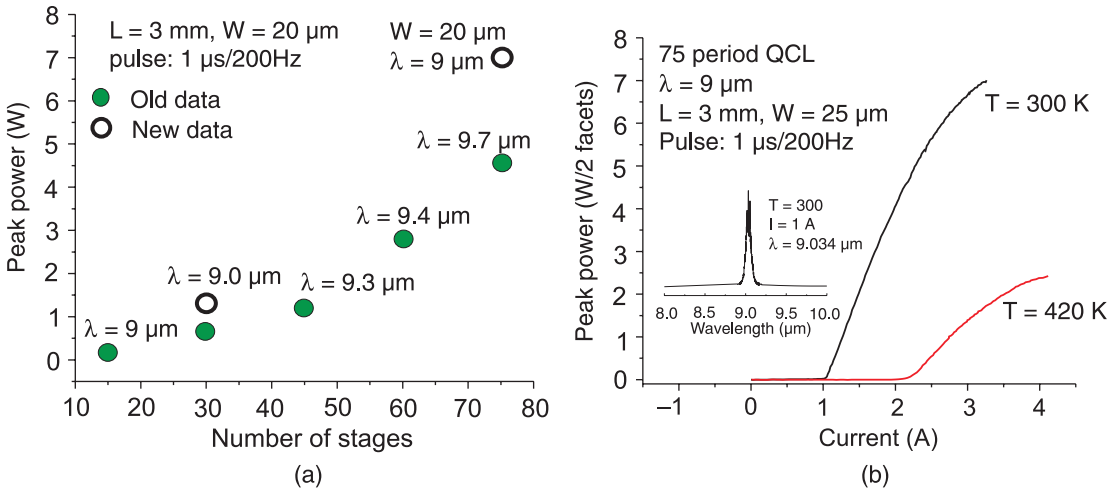

Fig.6. Peak power as a function of the number of stages for a series of 9–10 μm SLQCLs (a) and P-I behaviour of an 75-period QCL at λ = 9 μm (b).

guide, excellent material quality and careful processing of devices.

Figure 7 shows the average power per facet for a 30 and 75 period QCL as a function of duty cycle. Even though the 30 period device operates up to higher duty cycles, the 75 period device can still achieve higher average power thanks to its higher power slope efficiency. This data is uncorrected for a collection efficiency of ~85%. Over 300 mW was observed at 6% duty cycle for the 75 period device, which was the highest 300 K average power reported for a QCL at the time [9]. It should be noted that this ridge laser measurement was done with epilayer-up bonding of the laser to a copper heatsink.

6. Strain-balanced laser results

The minimum wavelengths demonstrated with $Ga_xIn_{1-x}As/Al_yIn_{1-y}As$ QCL technology has been 3.4 μm [10]. At slightly longer wavelength (3.54 μm), room temperature emission was reported with a threshold current density of only 1.2 kA/cm^2 but only a few mW of peak power [11]. Much more work has been done near λ = 5 μm, with threshold current densities as low as 1.7 kA/cm^2 and peak output power up to 1 W per facet [12,13].

More recently, a λ ~6 μm QCL was grown and fabricated using a $Ga_{0.41}In_{0.59}As/Al_{0.57}In_{0.43}As$ basis. The testing results are very impressive, as shown in Fig. 8(a). For only 30 periods, the maximum average power for a 3 mm by 21 μm cavity at room temperature is ~250 mW per 2 facets at a 10.5% duty cycle.

In order to more efficiently utilize the power emitted from the laser, a high reflectivity coating is required for the back mirror facet. Lasers were also cleaved into 1.5 mm cavities and coated with a Y_2O_3/Ti/Au (650 nm/20 nm/80 nm) to act as a high reflectivity mirror. This cavity length was used in order to benefit from the same threshold current density and total power conversion efficiency as demonstrated by the 3 mm laser, which was later confirmed

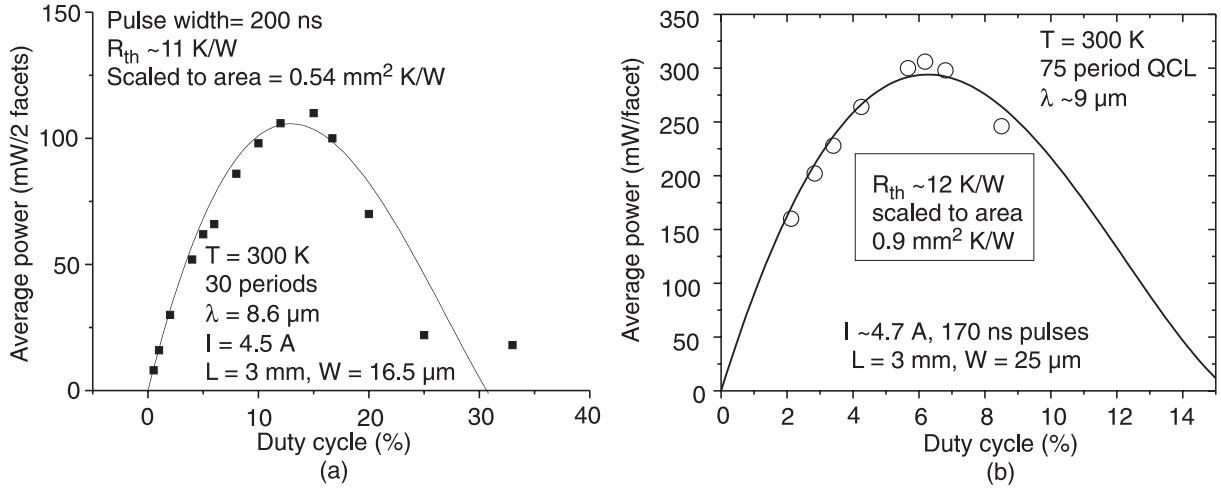

Fig. 7. Average power as a function of duty cycle for 30 and 75 period, 9 μm QCLs. The fit curve is used to calculate the thermal resistance and is based on pulsed device characteristics as a function of temperature.

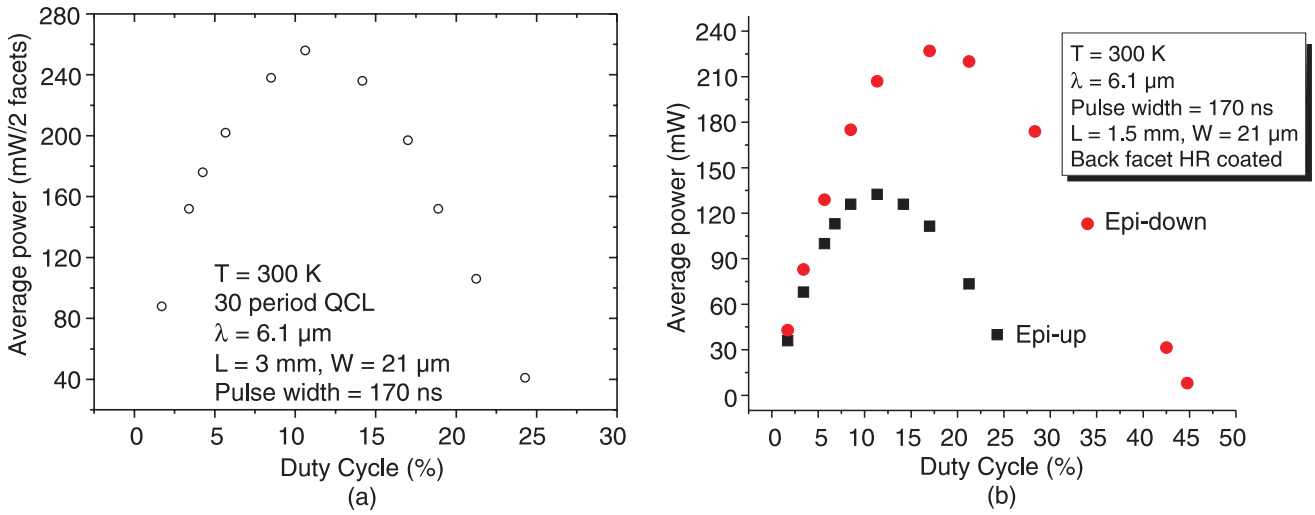

Fig. 8. Average power as a function of duty cycle for the same laser (a) and Average power per facet for epilayer-up and epilayer-down, 1.5 mm QCLs with the back facet HR coated (b).

during testing. In other words, the mirror reflectivity is very good (~98%), and this material is uniformly applicable as a coating for any laser in the 3–12 μm wavelength region.

This process also makes the laser a better candidate for epilayer-down bonding, thanks to the protected back facet. As shown in Fig. 8(b), average power measurements as a function of duty cycle were made for the coated 1.5 mm cavities in both the epilayer-up and epilayer-down configurations. The heat sink temperature was kept at 300 K. The epilayer-down device delivers 225 mW of average power out the uncoated facet at 17% duty cycle. At 45% duty cycle the average power is still 8 mW. As expected, the epilayer down configuration gives significantly more average power and operates at a higher duty cycle, thanks to a lower device thermal resistance. Further, the maximum average power from one facet is higher even than the best 9-μm result above, indicating that strain-balanced lasers can perform as well, or better, than their lattice-matched counterparts.

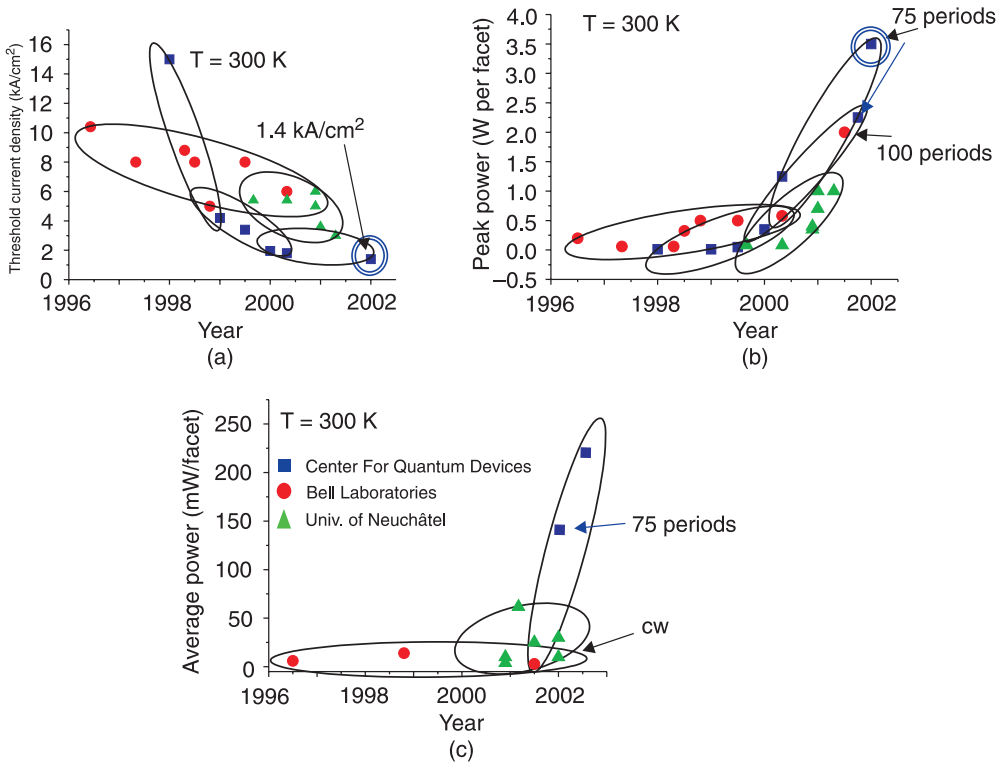

Fig. 9. Timeline of progress for λ > 4 μm quantum cascade laser technology with regards to room temperature threshold current density, peak output power, and average output power.

7. Timeline of progress

Single element performance has come a long way over the past few years. Two important parameters are charted in the figure below. Even at today's performance levels, with the proper packaging, QCL arrays should be capable of generating substantial peak powers at reasonable (> 5%) power conversion efficiency.

High duty cycle operation with high average power at most wavelengths still remains a challenge. Further, while pulsed mode operation at high duty cycle can be useful, a continuous wave source will enable the widest range of applications. For this reason, we must continue to refine both the material growth and packaging techniques.

This goal does involve some thermal management issues. Compared to near-infrared laser diodes, even the best uncooled QCLs operate with 5–10% power conversion efficiency. This is approximately 5–10 times less than comparable 808 nm pump lasers. Epilayer-down bonding and buried-ridge structures are the best hope in the short term for dealing with these issues.

The final answer to improving device efficiency lies ahead. The demonstration of the QCL is based on one-dimensional quantum confinement. The remaining two degrees of freedom impose limits on the carrier lifetime due to polar optical phonon scattering between subbands. It is this nonradiative process which limits the overall efficiency of the QCL. By implementing quantum wire and/or dot structures, it is theoretically possible to decrease the threshold requirements significantly. Demonstrating such a device is a lofty goal, but one well worth the effort.

8. Conclusions

In conclusion, the key technologies for demonstrating high power quantum cascade lasers have been explored. It is shown that, for strict control of material and fabrication technology, peak power in excess of 7 W is possible from a single 20 μm wide aperture. While lattice-matched layers can be used at longer wavelengths, strain-balancing has been shown to be a viable technique for realizing shorter wavelength QCLs. The high conduction band offset decreases thermal leakage and allows for higher duty cycle operation. The most straightforward example of this is an average power of 250 mW from a $\lambda = 6$ μm laser. Also, advances in mirror coating and epilayer-down die bonding are demonstrated, leading to even better device performance. Lastly, the current state of quantum cascade laser technology is discussed and some possible future research efforts are mentioned.

References

1. J. Faist, F. Capasso, D.L. Sivco, C. Sirtori, A.L. Hutchinson, and A.Y. Cho, "Quantum cascade laser", *Science* **264**, 553 (1994).
2. P. Yu and M. Cardona, *Fundamentals of Semiconductors*, Springer-Verlag, Berlin, 1996.
3. C. Sirtori, J. Faist, F. Capasso, D. Sivco, A. Hutchinson, and A. Cho, "Quantum cascade laser with plasmon-enhanced waveguide operating at 8.4 μm wavelength", *Appl. Phys. Lett.* **66**, 3242–3244 (1996)
4. C.G. Van de Walle, "Band lineups and deformation potentials in the model-solid theory", *Phys. Rev.* **B39**, 1871–1883 (1989).
5. C. Sirtori, J. Faist, F. Capasso, D.L. Sivco, A.L. Hutchinson, and A.Y. Cho, "Mid-infrared (8.5 μm) semiconductor laser operating at room temperature", *IEEE Photonics Techology. Lett.* **9**, 294–296 (1997).
6. G. Scamarcio, M. Troccoli, F. Capasso, A.L. Hutchinson, D.L. Sivco, and A.Y. Cho, "High peak power (2.2 W) superlattice quantum cascade laser", *Electronics Lett.* **37**, 295–296 (2001).
7. A. Matlis, S. Slivken, A. Tahraoui, K. J. Luo, J. Diaz, Z. Wu, A. Rybaltowski, C. Jelen, and M. Razeghi, "Low-threshold and high power λ ~9.0 μm quantum cascade lasers operating at room temperature", *Appl. Phys. Lett.* **77**, 1741–1743 (2000).
8. M. Beck, D. Hofstetter, T. Aellen, J. Faist, U. Oesterle, M. Ilegems, E. Gini, and H. Melchior, "Continuous wave operation of a mid-infrared semiconductor laser at room temperature", *Science* **295**, 301–305 (2002).
9. S. Slivken, Z. Huang, A. Matlis, A. Evans, and M. Razeghi, "High power (λ ~9 μm) quantum cascade lasers", *Appl. Phys. Lett.* **80**, 4091–4093 (2002).
10. J. Faist, F. Capasso, D.L. Sivco, A.L. Hutchinson, S.N.G. Chu, and A.Y. Cho, "Short wavelength (λ ~3.4 μm) quantum cascade laser based on strained compensated InGaAs/AlInAs", *Appl. Phys. Lett.***72**, 680–682 (1998).
11. F.Q. Liu, Y.Z. Zhang, Q.S. Zhang, D. Ding, B. Xu, Z.G. Wang, D.S. Jiang, and B.Q. Sun, "High-performance strain-compensated InGaAs/InAlAs quantum cascade lasers", *Semicond. Sci. Technol.* **15**, L44–L46 (2000).
12. S. Slivken, unpublished.
13. D. Hofstetter, M. Beck, T. Aellen, and J. Faist, "High-temperature operation of distributed feedback quantum-cascade lasers at 5.3 μm", *Appl Phys. Lett.* **78**, 396–398 (2001).

XV CONFERENCE ON LIQUID CRYSTALS

Chemistry, Physics and Applications

13–17 October, 2003

Zakopane

POLAND

The Conference is organized by Institute of Applied Physics and Institute of Chemistry of Military University of Technology Warsaw – Poland

The conference has been held every two years for 27 years. Since 1994 the conference has become the main forum for presentation and discussion of recent development in the field of liquid crystal research and technology of the region of East, West and Central Europe.

Sponsored by:

State Committee for Scientific Research (Poland)
SPIE – The International Society for Optical Engineering in association with SPIE /Poland Chapter
Polish Chemical Society

Conference Scientific Chair

Józef	ŻMIJA	Chairman
Roman	DĄBROWSKI	Co-Chairman
Jerzy	ZIELIŃSKI	Co-Chairman
Stanisław	KŁOSOWICZ	Secretary
Antoni	ADAMCZYK	
Danuta	BAUMAN	
Janusz	CHRUŚCIEL	
Krzysztof	CZUPRYŃSKI	
Grzegorz	DERFEL	
Jan	JADŻYN	
Jerzy	JANIK	
Jerzy	KĘDZIERSKI	
Bogdan	KOSMOWSKI	
Andrzej	MINIEWICZ	
Andrzej	ORZESZKO	
Zbigniew	RASZEWSKI	
Sylwester	RZOSKA	
Jan	STĄSIEK	
Jan	STECKI	
Stanisław	URBAN	
Stanisław	WRÓBEL	

Organizing Committee

Jerzy	ZIELIŃSKI	Chairman
Ryszard	CURYK	
Marek	OLIFIERCZUK	
Paweł	PERKOWSKI	
Wiktor	PIECEK	
Małgorzata	TUROS	

Institute of Applied Physics
ul. Kaliskiego 2
00-908 Warszawa
POLAND
Tel: +48 22 683-97-31, 683-92-62
Fax: +48 22 683-90-14, 683-95-69
email: zielj@wat.edu.pl
Web Site: http://strony.wp.pl/wp/clc2003/main.htm

Location and Conference Venue

The Conference will be held in Zakopane – the capital of Tatra Mountains. There is a convenient transportation from Warsaw and Kraków to Zakopane. Conference center, hotel and other facilities are located in the same building.

Conference will cover topics such as:

1. Synthesis and new materials.
2. Chiral phases, ferroelectric and antiferroelectric liquid crystals.
3. Macroscopic and microscopic properties – molecular dynamic.
4. Phase structure and phase transitions.
5. Electro- and thermo-optical effects: display devices and applications.
6. Polymer liquid crystals and composite structures.
7. Theory and molecular modeling.

Conference and hotel costs

Conference fee	500 PLN	(125 EUR)
Conference fee for students	300 PLN	(75 EUR)
Conference fee for accompanying person	300 PLN	(75 EUR)
Hotel (for 5 days with full board)		
Single room	1000 PLN	(250 EUR)
Bed in double room	800 PLN	(200 EUR)

Full board for participants, get together party, excursion, and banquet are included into conference fee and hotel cost.
Hotel reservation will be possible after prepaying.
A limited number of grants for students and young scientists partly covering the cost of the fee are available. Preference will be given to those presenting a paper.
Payments should be made in Polish currency, USD or Euro. For foreign participants cash payment at the conference desk without an additional charge will be possible after earlier organizers' approval.
The following possibilities are offered:
bank draft to:

Wojskowa Akademia Techniczna
00-908 WARSZAWA 49
P.B.H. Powszechny Bank Kredytowy S.A.
V Oddział Warszawa
11102018-422010001273
XV CLC – 2003

check to:

XV CLC – 2003
Wojskowa Akademia Techniczna
ul. Kaliskiego 2
00-908 WARSZAWA, POLAND

